Atom Indonesia

Journal homepage: http://atomindonesia.brin.go.id

Exploring the Effect of Different Scanning Protocols on the Modulation Transfer Function

H. Arjah[1,2], N. D. Osman[1*], H. ALMasri[3], C. Anam[4], M. E. Aziz[5]

[1]*Advanced Medical and Dental Institute, Universiti Sains Malaysia, Kepala Batas, Penang, Malaysia*
[2]*Radiology Department, Allmed Medical Center, Ramallah, Palestine*
[3]*Medical Imaging Department, Al-Quds University, Abu dis, Jerusalem, Palestine*
[4]*Department of Physics, Faculty of Sciences and Mathematics, Diponegoro University, Jl. Prof. Soedarto SH, Tembalang, Semarang 50275, Central Java, Indonesia*
[5]*Department of Radiology, School of Medical Sciences, Universiti Sains Malaysia, Kubang Kerian, Kelantan, Malaysia*

ARTICLE INFO

Article history:
Received 2 November 2024
Received in revised form 4 March 2025
Accepted 5 March 2025

Keywords:

Iterative reconstruction
In-plane resolution
IndoQCT
Brain filter
Modulation transfer function

ABSTRACT

The Iterative Reconstruction (IR) algorithm can enhance image quality and reduce patient dose. This study aims to evaluate the in-plane resolution (X- and Y-), in association with different IR and filtered back projection (FBP), on three different Computed Tomography (CT) scanners: General Electric (GE), Philips, and Siemens. Uniform water phantoms were scanned using 35 milligrays (mGy) and 65 (mGy) and then reconstructed using 2- and 5-millimetre (mm) slice thicknesses. Images were reconstructed using the iterative Beam Hardening Correction (iBHC), Sinogram-Affirmed Iterative Reconstruction (SAFIRE), 4th generation hybrid statistical iterative reconstruction proposed by philips (iDose^4), Filtered Back Projection (FBP), Adaptive Statistical iterative Reconstruction (ASiR-V), Weighted Filtered Back Projection (WFBP), Best Contrast or Brain Contrast algorithm (BC). All images were analysed using IndoQCT software. Automated Modulation Transfer Function (MTF) measurement was used to describe in-plane resolution. From the Siemens CT scanner findings, MTF at 10 % (MTF_{10}) was increased by applying the iBHC algorithm from 0.52 to 0.57, but MTF_{10} of SAFIRE and WFBP showed no difference. For the Philips CT scanner, the iDose^4 technique did not affect MTF_{10} compared to FBP, while the post-processing by BC decreases MTF_{10} from 0.5 to 0.49. For the GE CT scanner, the MTF is affected by radiation dose, while the ASiR-V MTF curve had no difference compared to FBP, with the highest MTF_{10} value of 0.67 for 35 mGy protocol compared to 0.64 for 65 mGy protocol. The image resolution is affected by CT dose and the use of reconstruction algorithms. These associated parameters may enhance or reduce image resolution.

INTRODUCTION*

High contrast spatial resolution is an essential parameter in CT and is assessed using MTF [1], MTF adopted by the Food and Drug Administration (FDA) as an index for image resolution and detector array performance [2,3]. It is related to image resolution, which describes the scanner's efficiency in detecting the space between two neighbouring points. The MTF represents the spatial equivalent of the frequency response of the imaging system [4] and determines how much contrast in the original object is maintained by the detector [5].

Currently, different CT scanner vendors have their proposed IR techniques, which are used to reduce patient dose and image noise and improve image quality at a lower radiation dose level than the needed dose level for standard FBP. Previous literature has determined the physical characteristics of CT images reconstructed by the new IR algorithm compared to classical FBP [6].

MTF equals the Fourier Transform (FT) for the Point Spread Function (PSF). The MTF is

*Corresponding author.
E-mail address: noordiyana@usm.my
DOI: https://doi.org/10.55981/aij.2025.1553

valuable for the linear system, whereas the IR and FBP are nonlinear systems. The MTF depends on multiple parameters such as radiation dose, slice thickness, and reconstruction algorithm. However, the MTF describes the resolution in the axial plane (X, Y). MTF is measured in line pairs per centimetre (lp/cm) or millimetre (lp/mm), and the size of (lp/cm) decreases as the frequency increases [7].

The MTF is a metric resolution system that describes object contrast recovery by the system as a spatial frequency function [8]. MTF is defined as the ratio of the output to input modulation and measures system response to different frequencies. The "ideal" system has a flat MTF curve. Mostly, the MTF rapidly degrades at higher frequencies. The limiting frequency can be achieved when the system response approaches zero. The spatial resolution related to MTF is the system's limiting resolution. A single MTF curve is achieved by averaging the MTF function over 360 degrees. MTF values at discrete locations in the MTF curve are used to evaluate the system response. CT system response evaluation often uses the 50 % MTF curve (MTF_{50}) or the MTF_{10}, which was used in this work. However, some researchers adopted the 0 % level of the MTF curve (MTF_0) [7]. MTF estimation of a CT system considers the reconstruction filter as an ideal ramp function multiplied by a cosine square window with its cutoff frequency at the CT system's Nyquist frequency [9]. The true MTF measurement exhibits the Nyquist frequency higher than the MTF value.

FBP is the process of estimating an object image slice from a set of projections. FBP is the most popular reconstruction algorithm used at present in CT applications [10]. However, Siemens uses WFBP [11], in which the WFBP signals are traced back through the volume to be reconstructed, converging toward the X-ray source. Therefore, the values are weighted with the squared reciprocal distance to the source. This makes the process look like the light cone of a pocket lamp. The distance is defined as the projection of the distance between the X-ray source and the current point to be reconstructed onto the central beam of the non-angulated fan [12]. However, new techniques used by CT vendors to enhance image quality, the Hybrid Statistical Iterative Reconstruction (HSIR) techniques applied on projection space and image space, combine both FBP and Iterative Reconstruction (IR) at different levels [13,14]. The iDose^4, SAFIRE, and ASIR-V are types of H/SIR. The BC algorithm is proposed to improve the differentiation between White Matter (WM), and Gray Matter (GM) [15]. However, the iBHC algorithm eliminates the beam hardening artifact [16].

This work aims to determine the effect of different brain CT protocols and parameters, such as the reconstruction algorithm, radiation dose, and slice thickness, on MTF. It did not aim to compare different vendors or scanner models.

METHODOLOGY

Scanners and protocols

Three CT scanners from 3 different vendors were employed in this work: Philips Ingenuity Core (Philips Healthcare, Cleveland, Ohio), which is equipped with FBP, iDose^4, and BC; Siemens SOMATOM® Go now (Siemens Healthcare, Forchheim, Germany), which is equipped with WFBP, iBHC, and SAFIRE; and GE Revolution™ (GE Healthcare, Milwaukee, WI), which is equipped with FBP and ASiR-V. Each scanner was evaluated using its phantom as shown in Fig. 1. Phantom scanning employed a head phantom of 16 cm and spiral mode. The MTF was evaluated using an automatic algorithm built into the IndoQCT software [17]. Five slices in a uniform water phantom were employed for MTF measurements, and the MTF curve was averaged from five slices. Brain filter was employed in the three CT scanners. Different radiation doses, slice thicknesses, and reconstruction algorithms were inspected to determine how these parameters affect the MTF.

Each scanner's phantom was scanned with two series of exposures using the standard protocol for brain CT, which uses 65 mGy volume Computed Tomography Dose Index ($CTDI_{vol}$), and the low-dose protocol, which uses 35 mGy. The scanned phantoms were reconstructed using different slice thicknesses and reconstruction algorithms according to Table 1. The phantoms were carefully scanned in the scanner isocenter. The Display FOV (DFOV) was kept as small as possible to eliminate MTF degradation due to a large DFOV. However, phantoms' sizes are different and hence need different DFOV so that MTF measurements will be differently affected [17]. This work aims to determine the effects of different algorithms on MTF for the same DFOV on the scanner rather than to compare different scanner MTFs.

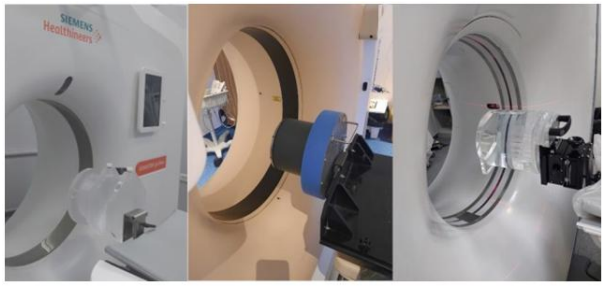

(a) (b) (c)

Fig. 1. Setup of a) Siemens scanner and phantom, b) Philips scanner and phantom, and c) GE scanner and phantom.

Table 1. Reconstruction algorithms and slice thickness used in each CT scanner for low-dose and standard-dose protocols.

Vendor	Siemens	Philips	GE
Model	SOMATOM® Go now	Ingenuity Core	Revolution ™
Algorithm	WFBP WFBP-iBHC SAFIRE SAFIRE-iBHC	FBP FBP-BC iDose^4 iDose^4-BC	FBP ASiR-V
Thickness	2 mm 5 mm	2 mm 5 mm	2.5 mm 5 mm

The employed filter in this work is the brain filter, which deals with the cupping artefact and shifts the MTF curve to the left part of the spectrum, and as a result, the resolution worsens [6,18,19]. The SOMATOM® Go Now CT scanner includes iBHC to eliminate beam hardening artefacts that appear beside the skull bone. In contrast, the Ingenuity Core scanner employs the BC algorithm to enhance the differentiation between White Matter (WM) and Grey Matter (GM). In contrast, the Revolution™ scanner does not use an extra algorithm for Brain CT.

MTF and Nyquist frequency calculation

The MTF is measured automatically by the IndoQCT software. The software algorithm measures the edge MTF without user intervention. The first step for the automated algorithm measurement is establishing the uniform water phantom centre by the centroid Eq. (1). The uniform water phantom edge is automatically contoured, and the automated algorithm draws a line from the phantom centre to the phantom edge. Then square Region of Interest (ROI) is selected at the edge of the phantom to determine the Edge Spread Function (ESF) as clarified in Fig. 2. The ESF curve is interpolated to get the Line Spread Function (LSF), which is Fourier transformed to calculate edge MTF [17], as shown in Fig. 3.

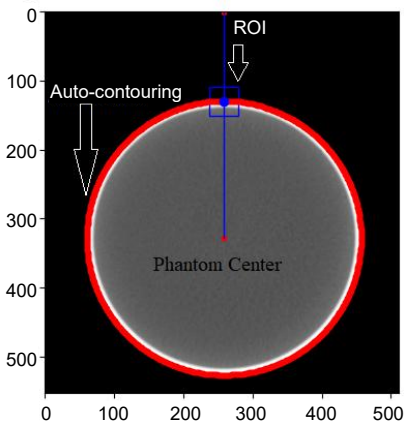

Fig. 2. Successful determination of phantom center, auto-contouring, and square ROI drawing by the automated algorithm.

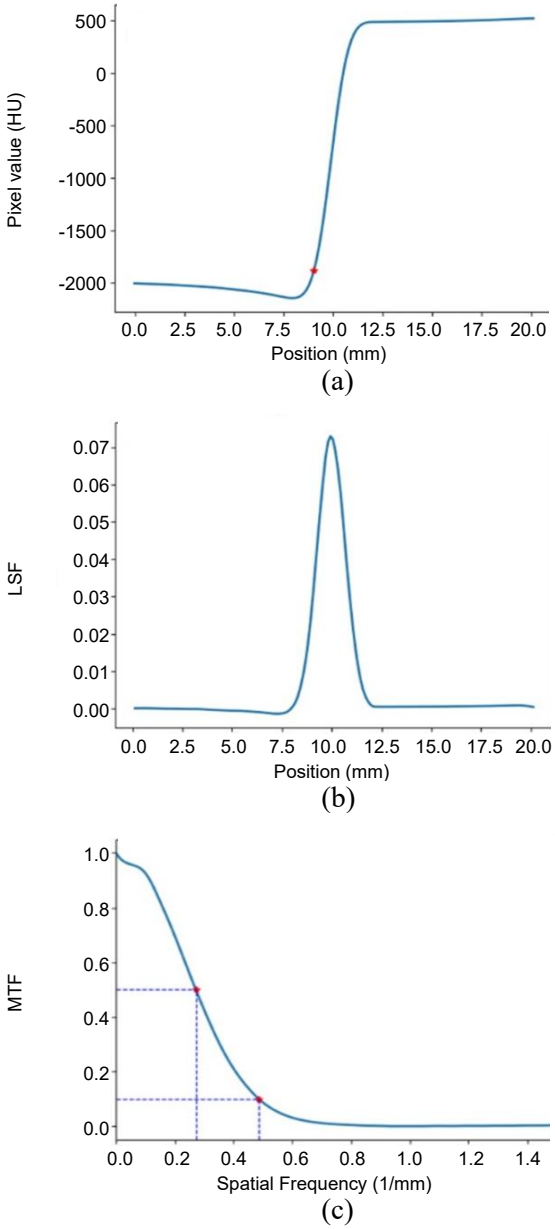

Fig. 3. Edge Spread Function (ESF) (a), which is interpolated to form the Line Spread Function (LSF) (b), LSF curve, which is Fourier transformed to provide a Modulation Transfer Function (MTF) (c).

The first step in MTF measurement is to determine the image center using the centroid Eq. (1).

$$(Xc, Yc) = \frac{1}{N}\sum_{i}^{n} = 1 \sum_{j}^{n} = 1 \, (Xi \, , \, Yj) \qquad (1)$$

Where X_C is the centre of the X-axis in the object, Y_C is the centre of the Y-axis in the object, N is the vector length, *i* is the X vector, *j* is Y vector, (X_i, Y_j) is the centre point which is formed by the cross product of X_C and Y_C or by the two vectors.

After the determination of (X_i, Y_j), the automated algorithm draws a line passing through the centre to the edge of the phantom and a square ROI on the edge of the phantom, as shown in Fig. 2. The average of the X value is used to calculate ESF, and the spline interpolation is applied to acquire four additional points between each pixel to obtain an interpolated curve for ESF, as shown in Fig. 3. The resulting curve is differentiated to form an LSF curve and forced to zero through the zeroing process to normalise the LSF to convert it to MTF, and then fix the 100 % MTF at zero spatial frequency. On the obtained MTF curve. The MTF_{10} and MTF_{50} are automatically determined. The MTF is equal to the Fourier transform of LSF according to Eq. (2) as follows.

$$X(k) = \sum_{j=0}^{n-1} X(j) e^{-i2\pi kj/N} \qquad (2)$$

Where K is a range from 0 to N-1, N is the LSF vector size. The MTF is used to form the Y-axis, and the X-axis is formed by spatial frequency according to Eq. (3).

$$\omega_S = \frac{1}{N_I \times I_S} \qquad (3)$$

N_I represents pixel number, and I_S represents sampling interval according to Eq. (4), which depends on the field of view (FOV). Eqs. (3) and (4) discuss why the MTF gets worse at higher DFOV. The spatial frequency is inversely proportional to I_S, which increases for larger FOV.

$$I_s = \frac{FOV}{512} \qquad (4)$$

Most researchers and this work adopt MTF_{10}. The diagnostic range of MTF_{10} should be higher than 0.5 [20].

RESULTS AND DISCUSSION

Siemens MTF

The MTF curves for Siemens images exhibit different positions according to the application of iBHC. This work includes 16 images for Siemens, which are differently reconstructed according to Table 1 from two scanning protocols, 35 and 65 mGy. In Fig. 4, the 4 curves for 2-mm and 5-mm images scanned using both protocols are divided into two overlapped groups, each overlapped group at a specific position in the Cartesian diagram. The right side overlapped curves group was reconstructed using iBHC, while the left side overlapped group was reconstructed without iBHC. The different radiation doses and slice thicknesses exhibited the same MTF curve; the only factor that affected Siemens MTF was the iBHC. However, theoretically, the right curves possess a more efficient system response and higher MTF_{10} [7].

The two groups of MTF curves mentioned in Fig. 4 exhibit different MTF_{10}. The images reconstructed without iBHC possess an MTF_{10} equal to 0.52. while the application of iBHC enhanced image resolution and increased the MTF_{10} to 0.57. However, other parameters such as SAFIRE level 4 (S4), WFBP, radiation dose, and slice thickness did not affect MTF_{10}.

The application of S4 does not affect MTF_{10}. The same results were noticed by Ghetti C et al. [21] in their work, which concluded that there is no difference in MTF between the WFBP and SAFIRE. Also, no significant difference was noticed for different radiation doses and slice thicknesses. While using iBHC enhances the MTF and provides a higher MTF_{10}, the MTF_{10} for WFBP and SAFIRE was 0.52. The use of iBHC increased the MTF_{10} for the head filter to 0.57.

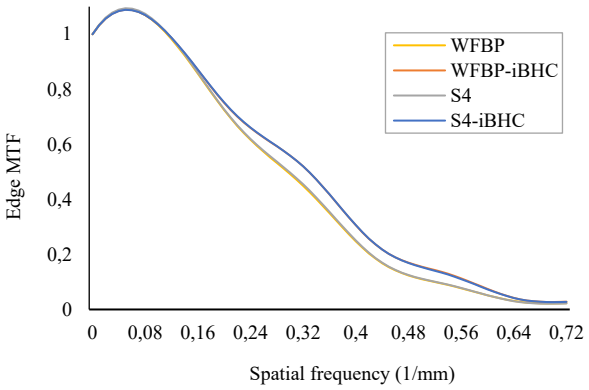

Fig. 4. MTF curve for Siemens images reconstructed using different algorithms and slice thickness, for phantoms scanned using low dose and standard protocols.

The iBHC consists of four steps; the first step is the X-ray projections prefiltration [22]. This process enhances the image resolution. The increased resolution is due to the narrowing of the X-ray spectrum and, therefore, less Signal-to-Noise Ratio (SNR), and hence higher resolution [23]. The plotted curves show separation into two groups. The left side curves were reconstructed without iBHC, and the application of iBHC moved the curves to the right. This implies that iBHC enhances image resolution.

The SAFIRE algorithm includes noise subtraction, a denoising process that includes smoothing for low-dose noise images. However, the smooth image exhibits less resolution [15]. The SAFIRE algorithm degrades image noise while preserving spatial resolution [11]. Preserving spatial resolution maintains MTF_{10}, producing no difference between SAFIRE and WFBP.

Philips MTF

The MTF curves for Philips show differences according to the application of the BC post-processing algorithm, while the slice thickness and radiation dose don't affect the MTF curve. This work includes 16 images for the Philips scanner reconstructed differently, as illustrated in Table 1. The obtained MTF curves are presented in Fig. 5 for 2- and 5-mm images scanned using the 35 mGy and 65 mGy protocols. The MTF curve worsened and shifted to the left for images post-processed by the BC algorithm. However, the BC algorithm slightly worsens the MTF curve, and the obtained curves overlap, which means the images exhibit nearly the same resolution.

The MTF_{10} is equal to 0.5 for iDose^4 and FBP, while the application of BC reduces it to 0.49. The slice thickness and radiation dose have no effect on MTF_{10}, and BC can be considered the main parameter that worsens image resolution; however, this is a slight worsening, but should be taken into account because the diagnostic range of MTF in CT scanners should be equal to 0.5 or higher.

iDose^4 algorithm modifies the projection data to correct the noisiest measurements due to poor SNR. The image resolution and edge are preserved. The subsequent processing step in image space includes noise estimation and noise subtraction, as clarified by the iDose^4 white paper [24]. iDose^4 white paper shows that the iDose^4 shifts the MTF curve to the right, and reducing radiation dose with the use of iDose^4 preserves the MTF curve or shifts it to the right [24]. However, the filter discussed in the iDose^4 white paper is filter C, while the filter assessed in this work is the brain filter. The iDose^4 enhances image quality and minimises image noise. However, noise reduction worsens MTF_{10} [12], while edge preserving maintains MTF_{10}.

The BC algorithm is a post-processing algorithm used by Philips [24]. This algorithm modifies the CT number to increase the difference between WM and GM [25]. The BC algorithm has benefits such as enhancement of Contrast-to-Noise Ratio (CNR) and drawbacks such as modified CT numbers. This work shows an additional drawback of the BC algorithm: It generally degrades image resolution. This degradation is considered because the MTF_{10} is lower than 0.5, which is unacceptable in CT.

GE MTF

The MTF curves for GE show differences according to the radiation dose, while the reconstruction algorithm and slice thickness do not affect the MTF curve. This work includes 8 images for the GE scanner reconstructed differently for two scanning protocols, 35 and 65 mGy; the MTF curves are illustrated in Fig. 6. The curve's position shows that lowering the radiation dose is the main parameter that enhances image resolution. The plotted MTF curves for 2.5-mm images exhibit the same approaches as 5-mm images. The curves and slice thickness were independent of the reconstruction algorithm. The standard dose and low dose protocols MTF curves overlap at frequency 0.83 l/mm which exhibits the same resolution.

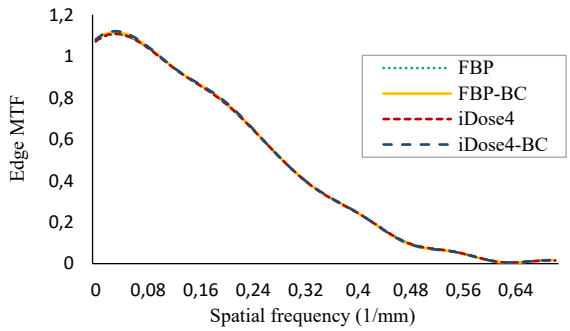

Fig. 5. MTF curve for Philips images reconstructed using different algorithms, and slice thickness and scanned using low-dose and standard protocols.

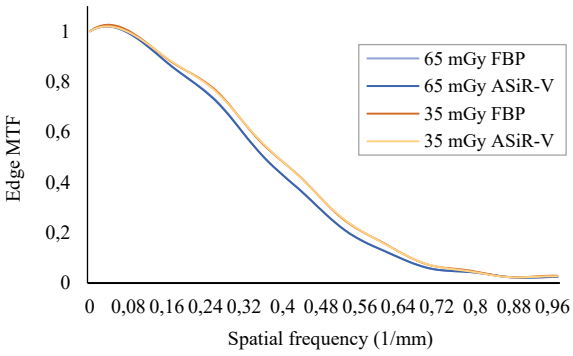

Fig. 6. MTF curve for GE images reconstructed using 5-mm slice thickness, and using different algorithms and scanned using low dose and standard protocols.

The MTF_{10} of the GE scanner is solely affected by radiation dose and is independent of slice thickness and reconstruction algorithm. The MTF_{10} for the 35 mGy protocol equals 0.67, while the MTF_{10} for the 65 mGy protocol equals 0.64.

The same finding was noticed by Friedman et al. (2013), which shows that the MTF is dose-dependent [26]. The slice thickness and reconstruction algorithm did not affect the MTF curve. Image processing by the ASiR-V algorithm includes initial image reconstruction by FBP to estimate the object, and then incorporates the object model to adjust the image [27]. This process does not affect the MTF curve. As mentioned by the ASiR-V white paper, the algorithm preserves spatial resolution while decreasing image noise, and this discusses the overlapped MTF curves of ASiR-V and FBP images.

Hussain et al.'s work on MTF curves for the low-dose protocol was better than MTF curves acquired by the full-dose protocol [28]. The MTF curve exhibits MTF independence of the reconstruction algorithm, and lowering the radiation dose shifts the curves to the right. However, MTF is not influenced by exposure parameters [29].

MTF curves are affected by the detector array [30], reconstruction filter [31], and radiation dose [32]. These parameters vary between scanners. However, the MTF_{10} should not be lower than 0.5, and different scanner types should provide $MTF_{10} \geq 0.5$. SOMATOM® Go Now and Revolution™ MTF_{10} values show $MTF_{10} > 0.5$, while the Ingenuity Core scanner MTF_{10} is equal to 0.5 and minimized to 0.49 after BC post processing.

The signal and resolution have an inverse relationship [21]. The MTF_{10} results imply that the IR preserves image resolution in all scanners, and the IR, compared to FBP, exhibited the same resolution.

CONCLUSION

According to the manufacturer, MTF curves are affected by multiple factors. The use of different reconstruction algorithms, different radiation doses, artifact reduction techniques, and post-processing algorithms could enhance or worsen the MTF curve. For Siemens, the iBHC enhanced the MTF, while in Philips, the BC algorithm worsened it. In contrast, the reconstruction algorithm does not modify the MTF curve in GE, and lowering the radiation dose improved the resolution and shifted the MTF curve to the right.

ACKNOWLEDGMENT

The authors acknowledge the radiology departments that allowed us to use their scanners to complete this work and the developer of IndoQCT software for their free license and beneficial training on the software.

AUTHOR CONTRIBUTION

H. Arjah, N. D. Osman, H. ALMasri, C. Anam, and M. E. Aziz equally contributed as the main contributors of this paper. All authors read and approved the final version of the paper.

REFERENCES

1. C. Anam, T. Fujibuchi, F. Haryanto *et al.*, Pol. J. Med. Phys. Eng. **25** (2019) 179.
2. B. W. Pogue, T. C. Zhu, V. Ntziachristos *et al.,* Med. Phys. **51** (2024) 740.
3. E. Karali, C. Michail, G. Fountos *et al*., Cryst. **14** (2024) 416.
4. P. Bhattacharya, R. Fornari, and H. Kamimura, Comprehensive Semiconductor Science and Technology, Elsevier, Oxford (2011).
5. S. N. Ahmed, Physics and Engineering of Radiation Detection, Elsevier Science, Amsterdam (2014).
6. N. Paruccini, R. Villa, C. Pasquali *et al.,* Physica Med. **41** (2017) 58.
7. E. Seeram, Computed Tomography Physical Principles, Clinical Applications and Quality Control, 4th ed., Saunders, Philadelphia (2015).
8. E. Samei, D. Bakalyar, K. L. Boedeker *et al.*, Med. Phys. **46** (2019) e735.
9. J. Hsieh, Computed Tomography: Principles, Design, Artifacts and Recent Advances, Spie Press, Bellingham, Washington **(**USA) (2015) 1.
10. M. T. Al Hussani and M. H. A Al Hayani, Coll. Eng. J. **17** (2019) 151.
11. K. Grant, R. Raupach, White Paper (2012) 1.
12. T. Pan, J. Nucl. Med. **50** (2009) 1194.
13. J. Greffier, J. Frandon, A. Larbi *et al*., Diagn. Inte rventional Imaging **100** (2019) 763.
14. D. Qiu and E. Seeram, Radiol: Open J. **1** (2016) 42.
15. M. N. Bongers, G. Bier, C. Schabel *et al*., Invest. Radiol. **54** (2019) 98.

16. D. A. Zarakovitis and A. G. Karametos, SN Compr. Clin. Med. **7** (2025) 35.

17. C. Anam, T. Fujibuchi, W. S. Budi *et al.,* J. Appl. Clin. Med. Phys. **19** (2018) 244.

18. F. R. Arisyi, C. Anam and C. E. Widodo, Int. J. Sci. Res. Sci. Technol. **8** (2021) 396.

19. D. Pesolillo, Image Quality and Dose Evaluation of Filtered Back Projection Versus Iterative Reconstruction Algorithm in Multislice Computed Tomography, Alma Mater Studiorum, University of Bologna, 2015.

20. S. J. O. Rytky, A. Tiulpin, M. A. J. Finnilä *et al*., Ann. Biomed. Eng. **52** (2024) 1255.

21. C. Ghetti, F. Palleri, G. Serreli *et al.,* J. Appl. Clin. Med. Phys. **14** (2013) 263.

22. R. Bock, S. Hoppe, H. Scherl *et al*., *Beam Hardening Correction with an Iterative Scheme using an Exact Backward Projector and a Polychromatic Forward Projector.* in: Bild. Für Die Medizin 2007, Springer Berlin Heidelberg, Berlin, Heidelberg (2007) 46.

23. P. Jin, C.A. Bouman and K. D. Sauer, IEEE Trans. Comput. Imaging **1** (2015) 200.

24. Philips, IDose^4 Iterative Reconstruction Technique, Whitepaper (2011).

25. Hamza, N. D. Osman, M. Z. Ahmad *et al*., Radiogr. **28** (2022) S2.

26. S. N. Friedman, G. S. K. Fung, J. H. Siewerdsen *et al*., Med. Phys. **40** (2013) 1.

27. C. T. Jensen, X. Liu, E. P. Tamm *et al.,* Am. J. Roentgenol. **215** (2020) 50.

28. F. A. Hussain, N. Mail, A. M. Shamy *et al.*, J. Appl. Clin. Med. Phys. **17** (2016) 419.

29. L. E. Lubis, I. Hariyati, D. Ryangga *et al.,* Atom Indones. **46** (2020) 69. (in Indonesian)

30. L. Masturzo, P. Barca, L. De Masi *et al.*, Eur. Radio. Exp. **9** (2025) 1.

31. C. Anam, A. Naufal, L.E. Lubis *et al.,* Physica Med. **129** (2025) 104876.

32. B. S. Wulandari, C. Anam, H. Sutanto *et al.,* Int. J. Sci. Res. Sci. Technol. **11** (2024) 349.